Towards a mathematical taxonomy of visual illusions?

W.A. Kreiner Faculty of Natural Sciences University of Ulm

Basic functions used in fitting procedures

y(x)=	Power x^(-1) 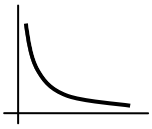	Expon. decay exp(-B·x) 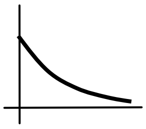	Linear D+A·x 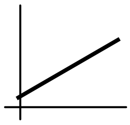	Lognormal exp[-(ln x)^{2}] 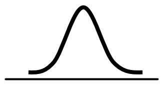	Trigonometric cos(4·(x-S2)) 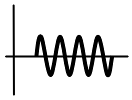
page					
Baldwin 16, 18	●	●	○		
Café wall 9				●	
Checkerboard 14	●	●			
Delboeuf 5, 23	●	●	○		
Müller-Lyer 20		●	○		
Oppel-Kundt 30					
Poggendorff 7, 10, 26		●	○		●
Size constancy 3, 11, 13	●				
Split circle 28	●				
Zöllner 6, 25		●	○		

1. Introduction

The front page shows a variant of the Müller-Lyer illusion: The corners of the tall white triangles facing each other (top) appear to be farther apart than the apices of the long red triangles (bottom). Actually, the spacing is the same. The question arises whether an algebraic expression can be found approximating the perceived spacing as a function of one independent variable, well within the experimental error limits.

Any perception may be called an illusion in the sense that the visual system does not employ absolute units when, for example, judging an object or distance as being large or small. However, varying a certain parameter (eg, the angle at the apex of the triangles or of the fins in the classic Müller-Lyer illusion), it turns out, that the distance between the apices appears to vary in a quite systematic way. Putting on the results over the parameter chosen one usually finds that the experimental values, beside some scatter, seem to follow a smooth function.

On measuring the magnitude of a visual illusion as a function of a particular variable, its value is usually varied in steps of equal size over the course of the experiment. The experimental results are plotted on a diagram, together with their standard deviations, and it is common practice to connect them by straight lines which give an impression of the general trend and the characteristic features of the illusion. Occasionally, this is called a signature (Ninio and O´Regan, 1999).

Psychophysical experiments on visual illusions help to narrow down the range of possible causes of an illusion. Assuming that visual data processing is based on specific neurophysiological mechanisms, one may set up a conceptual model for each of the illusions from which a hypothetical explanation can be derived as well as an algebraic function approximating the experimental values. It turns out that in case of some of the illusions just one of quite simple expressions serves the purpose, eg, an exponential decay function or a lognormal function. One may call them basic functions. Other illusions can be approximated only by a combination of several functions, indicating that there may be more than one of so called basic effects involved. However, comparing different illusions, one may check whether they partly share the same basic functions. This may be useful with regard to the question whether these illusions may be partly based on the same effects and possibly share similar features of data processing.

Coren, Girgus, Erlichmann, and Hakstian (1976) published a classification system for visual-geometric illusions, based upon the interrelationship between behavioral responses to various distortions, employing forty five illusion configurations. They also report on earlier attempts to classify geometric visual illusions.

2. Basic Functions

As already mentioned, in case of some of the illusions, the experimental values can be approximated within the error limits by a fairly simple algebraic expression, eg, by an exponential decay function or even a linear function. One may assume that they correspond to certain mechanisms in the context of visual data processing. However, from these basic functions more complicated expressions can be built up, suitable to describe illusions where several effects seem to be involved, interacting as well as opposing effects. In the following, examples of simple functions are given, each of them approximating either one particular geometric visual illusion or one particular effect contributing to one of the more complex illusions.

2.1 Power function

As experiments show, a change in the size of the retinal image of an object does not necessarily result in a proportionate change of its perceived size (Schur, 1925; Gilinsky, 1955). To give an example, the diameter y of the retinal image of a simple geometrical object, eg, a circular line, will shrink with increasing distance of observation x, following the power function y(x) ~ x^(-1), due to a law of geometrical optics (Fig. 1, lower curve). However, in general, the perceived size will not shrink quite as rapidly. This is known as size constancy.

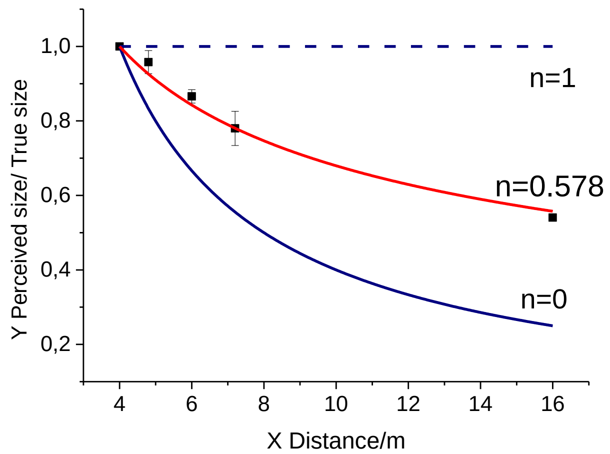

Fig. 1
Red curve: Perceived diameter of a bright disk as a function of the distance of observation (in horizontal direction, independent variable x, in meters).

Functions:
upper curve: y= (x/d0)^(n-1)
Results of fitting:
n= 0.578(22)
Chi^2/DoF= 0.00046
R^2 = 0.98614

lower curve: y= (x/d0)^(-1)
(no size constancy, retinal image)

The perceived shrinking effect can be approximated by adding a parameter, n, to the exponent of the independent variable, leading to y(perc, x) ~ x^(n-1) (Kreiner, 2004). The underlying conceptual model is based on the idea that the visual system selects a section of limited size from the retinal image for data processing in order to produce the perceived image. The size of this conspicuity range chosen will be reduced progressively as soon as the structure of interest gets finer with increasing distance of observation while the data processing and storage capacity stays constant, leading to an enlarged apparent image. The data In Fig. 1 refer to an experiment performed by Schur (1925). She measured the perceived size of a bright disk seen in the dark while the distance of observation was varied between 4.8m and 16m (red curve in Fig. 1). The function employed for the fitting procedure is y(x) = (x/d0)^(n-1), where the d0=4 in the denominator indicates that the experimental values found for the perceived size are standardized to the apparent size of the reference disk which was to be seen at a constant distance of 4 meters.

As a result, a size constancy parameter of n=0.578(22) was found. The dashed blue horizontal line corresponds to n=1, [y(x) = (x/d0)^0 = 1 = const.], which means that the apparent size would stay the same for any distance of observation. The blue lower curve gives the perceived size in the absence of any size constancy effect (n=0), simultaneously corresponding to the size of the retinal image as a function of distance.

This power function is suitable do describe all possible degrees of size constancy, just by varying the parameter n between 0 and 1. This parameter determines the slope of the function telling the magnification, ie, the apparent size relative to the retinal image at any distance. As shown later, this concept of a variable conspicuity range can be applied to related illusions as well, where, eg, a triangle or a stroke pattern stay at constant distance, but reduce in size, so the information density (fineness of structure) increases. See Chapter 4, Variants of size constancy.

2.2 Exponential decay function

The typical exponential decay function starts from a maximum value at x=0, first decreasing rapidly, but then approaching the x-axis slower and slower.

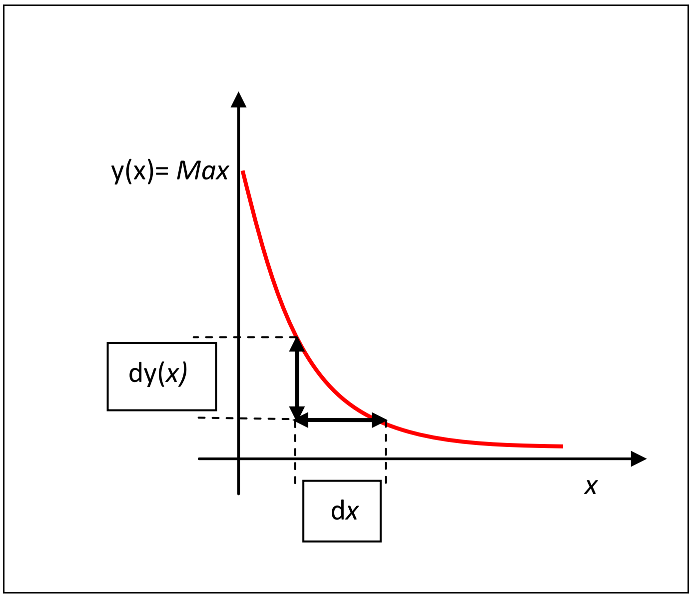

Fig. 2
Exponential decay function

2.2.1 A variant of the Delboeuf Illusion (Fig. 3) may serve as an example. Skinner and Simmons (1998) report that the apparent size of the small square depends on its position in relation to the larger one. It appears largest in a concentric position, but the magnitude of the effect decreases as soon as it moves out of center. The authors investigated the perceived size of the small square (the target T) in relation to a larger one (L). The diagram in Fig. 3 shows the apparent size of the target as a function of the displacement x. Out of the six values obtained by the authors, only the first four are shown where T is at least partly overlaps L, forming a conceptual unity.

Fig. 3 Delboeuf illusion on two squares. The experimental values refer to the perceived size of the target T (the smaller square) as a function of its position relative to L. Data from Skinner and Simmons (1998).

Function fitted:
y = 4.3·exp(-B·x)

The factor 4.3 means the maximum illusion (in mm), at x=0.

Results of fitting:
B= 0.00469(48)
Chi^2/DoF = 0.04713
R^2 = 0.97959

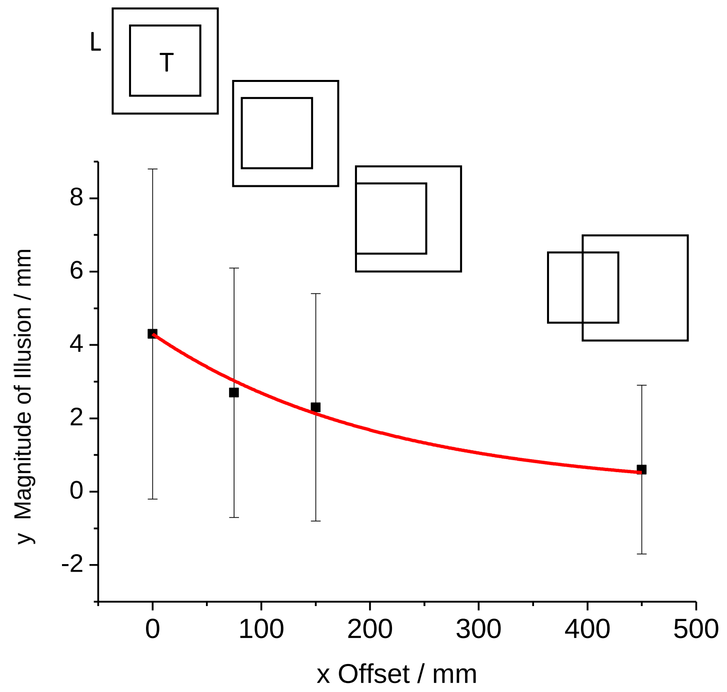

The exponential decay function fitted can be derived from a model in the following way: Maximum Illusion occurs when T and L are exactly concentric. This supports the conclusion that it is based on the impression of symmetry and coherence, leading to closer inspection which triggers a size constancy effect. A small shift would already distort it considerably, causing a fairly strong effect, ie, a decrease of apparent size. However, the same shift, applied to squares already out of center, has a considerably smaller impact. This leads to the differential equation:

$$d(magnitude) = -B \cdot magnitude \cdot d(offset) \quad \text{or} \quad \frac{d(magnitude)}{magnitude} = -B \cdot d(offset) \qquad (1)$$

In other words: An infinitely small decrease of the illusion [*d(magnitude)*] is in proportion the actual *magnitude* times an infinitely small offset of the squares [*d(offset)*]. *B* means a parameter to be fitted from the experimental date. This is called a differential equation. Integration leads to

$$\int \frac{d(magnitude)}{magnitude} = -B \cdot \int d(offset) + C \quad \text{--->} \quad \ln(magnitude) = -B \cdot offset + C \qquad (2)$$

The constant of integration C can be found from choosing $offset$ = 0. In this case, both squares are concentric and the magnitude of the illusion is at its maximum, C= $\ln(Max)$. From Eq (2):

$$ln\frac{(magnitude)}{(Max)} = -\text{B}\cdot(\text{offset}) \qquad \text{or} \qquad \boxed{magnitude \; = Max \cdot e^{-B\cdot(offset)}\;.}$$

This function, the solution of the differential equation, describes an exponential decay of the illusion with increasing offset between the target square (T) and the inducing square (L).

2.2.2 Zöllner Illusion. Luminance contrast

This example refers to the effect of the luminance on the magnitude of the Zöllner (1860) illusion (Li and Guo, 1995). The goal was to measure the error in estimating the parallelness of adjacent lines as a function of the contrast. The error was found to approach a constant

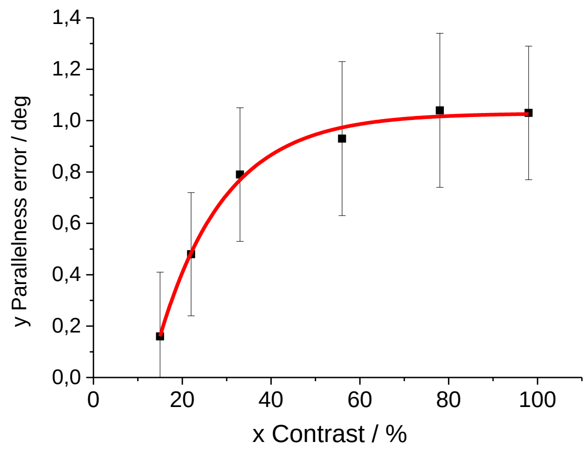

Fig. 4 Effect of luminance contrast on the magnitude of the Zöllner illusion. Data from Li and Guo (1995).

Function: y= D-A·exp(-B·x)

Parameters Fitted:

D= 1.029(22)
A= 2.37(27)
B= 0.0670(72)

Chi^2/DoF= 0.00098
R^2 = 0.99524

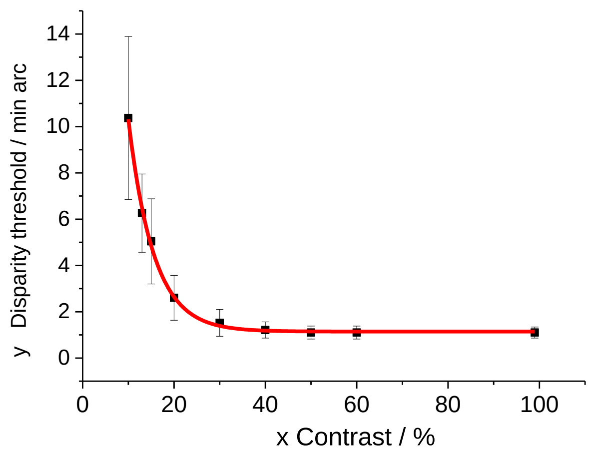

Fig. 5 Effect of luminance contrast on stereoscopic threshold.

Function:
y=D+A·exp(-B·x)

Parameters obtained

D= 1.143(63)
A= 56.0(38)
B= 0.1810(63)

Chi^2/DoF= 0.01815
R^2 = 0.99871

value D (Fig. 4). The same authors investigated the effect of the luminance contrast on the stereoscopic threshold (Fig. 5). In Fig. 6 the exponential parts of each function are compared.

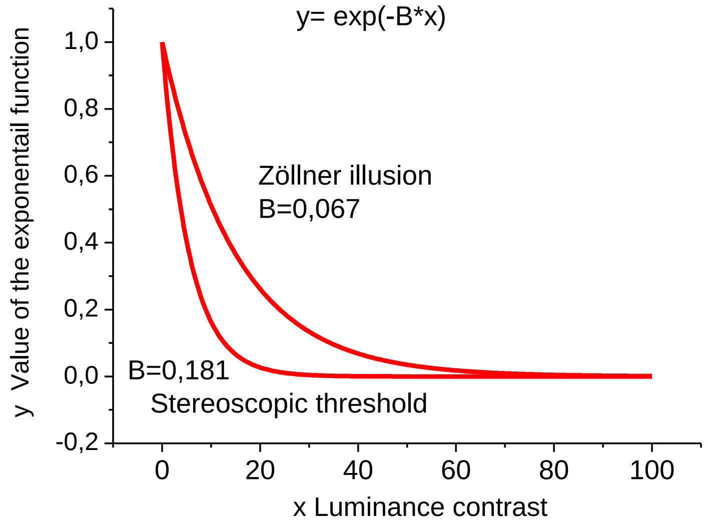

Fig. 6 Comparison of the two exponential functions only.

Function :
y= exp(-B·x)

Corresponding to the larger B-value, the function characterizing the stereoscopic threshold approaches the limit considerably faster.

In case of the influence of the luminance contrast on the Zöllner illusion the function is smoother, indicating that the maximum effect is approached slower than in case of the stereoscopic threshold.

2.3 Linear function

Fig. 7 gives a variant of the Poggendorff illusion, investigated by Wenderoth, Beh, and White (1978). There is an oblique black test line and a vertical inducing line at its right end. There were five dots in a row at each end of the line, out of which only one was presented at a

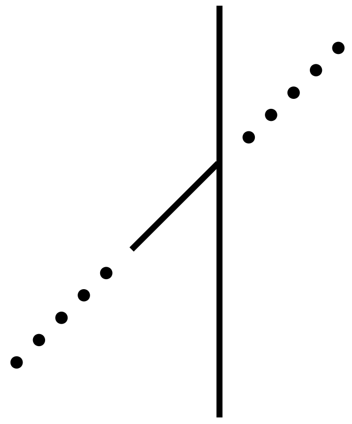

Fig. 7 A variant of the Poggendorff illusion. The ten dots are aligned with the oblique test line. In the experiment only one dot was shown at a time. The goal was to determine the point of subjective alignment.

time. In the experiment, line-dot alignment errors were measured. The goal of the experiment was to measure the point of subjective vertical alignment at each of the ten horizontal coordinates. It turned out that the subjects shifted the dots slightly towards the horizontal in order to achieve alignment. The effect is less pronounced near the open end of the oblique line, but seems to be enhanced by the vertical inducing line. However, in any case the perceived vertical offset depends linearly on the distance from the end of the test line. Fig. 8 (below) gives the perceived positions of the dots where they appear to be aligned. The grey line gives the true extension of the test line. A linear function D + A*x can be fitted to the subjective positions of the dots. The results are:

Table 1	dots near left tip	dots near vertical line
D	– 1.43(31)	– 0.28(14)
A	0.888(12)	0.756(12)

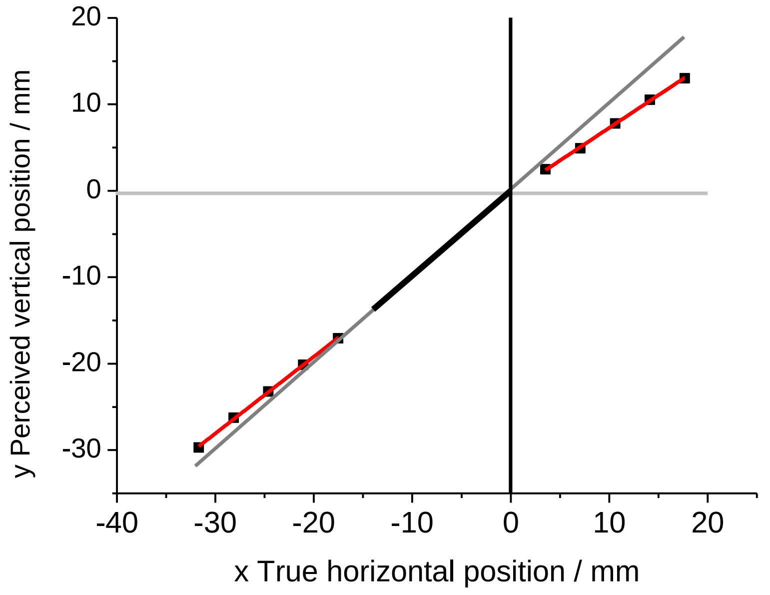

Fig. 8
Subjective line-dot alignments. The subjective vertical offset is proportional to the distance from the end of the test line. Fit of the function y(x) = D+A*x.

The true position of the dots is along the **grey** oblique line.

The Baldwin, the Müller-Lyer, and the Delboeuf illusion have one effect in common called averaging. Two geometric elements of different extension seem to influence each other such that the element of larger extent appears to shrink slightly and vice versa. For the contribution of a linear function see chapters 4.2, 4.3, 4.4.

2.5 Lognormal function

In the café wall illusion black and white rectangles arranged in rows appear wedge shaped (Fraser, 1908; Gregory, 1977). In the version shown below (Fig. 9) only one kind of shadowed tiles is employed. In the version investigated each tile was framed by a narrow

Fig. 9

Basic pattern. The middle row is slightly shifted with respect to the rows above and below.

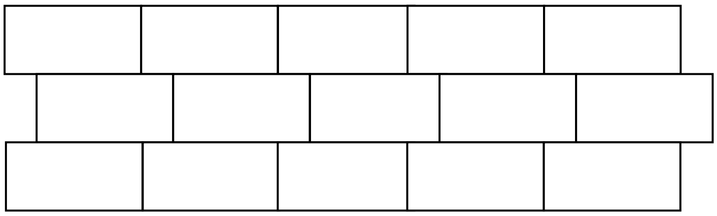

The tiles are shaded from white to black and to white again. The border lines of the rectangles are omitted.

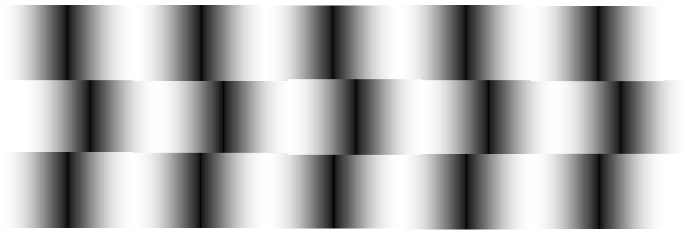

Inserting two grey lines (as shown to the right)

in between two rows (as indicated by the arrows) causes the tiles of the middle row to appear wedge shaped.

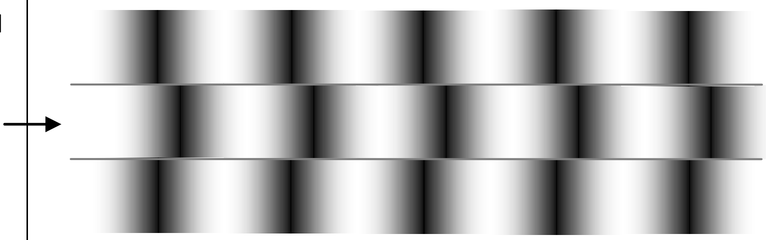

Fig. 10 Magnitude of the Cafè wall illusion as a function of the width of the framing line of shadowed rectangles. Semi-logarithmic plot. 40% grey refers to the darkness of the line separating the rows of tiles. The green bar indicates the resolution limit of the eye (one min arc = 2.91E-4 rad). The maximum illusion occurs at a line width clearly below this limit.

Function:
y = A*exp[-B*(log(x/C)^2)]

Parameters fitted:
A= 59.7(26)
B= 0,527(63)
C=1.549(81)

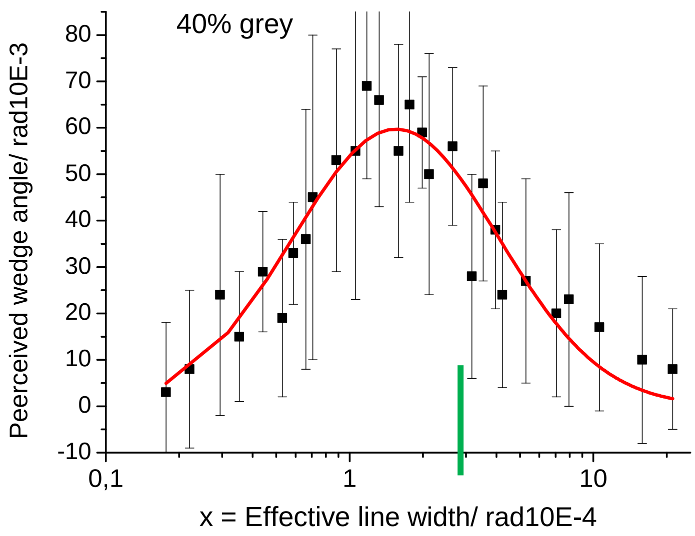

grey line, its width being the independent variable x (Kreiner, 2008; 2012). Starting from zero line width (at x= -∞, on a logarithmic scale), there will be no wedge illusion. Plotting the magnitude of the illusion as a function of the line width (in deg arc) one finds that it first increases and then, after having passed through a maximum, decreases again towards x= ∞. Plotted over a linear scale of the line width, this curve exhibits an asymmetric shape and can be approached by a lognormal function: $y(x) = \sim \exp[-(\ln x)^2]$. In Fig.10 it is shown in a semi-logarithmic plot. It turns out that the maximum illusion occurs at a line width definitely below the resolution limit of the eye (which is at about 1 min arc). In addition, the magnitude of the illusion depends on the luminance contrast of the framing line as well, so does the exact position of the maximum. In the example given darkness was 40%.

2.4 Trigonometric function

The degree of an illusion may depend on the orientation of the stimulus, as it has been observed on the Poggendorff illusion by Weintraub and Krantz (1971, 1980). Weintraub, Krantz, and Olson (1980) found that the magnitude of the Poggendorff illusion oscillates following a sinusoidal function.

Trigonometric functions are suitable to describe periodicity. Rotating the stimulus by 360^0 will again produce the same result, but the curve determined experimentally may exhibit features repeating after rotation of 90^0 as well (Fig. 11).

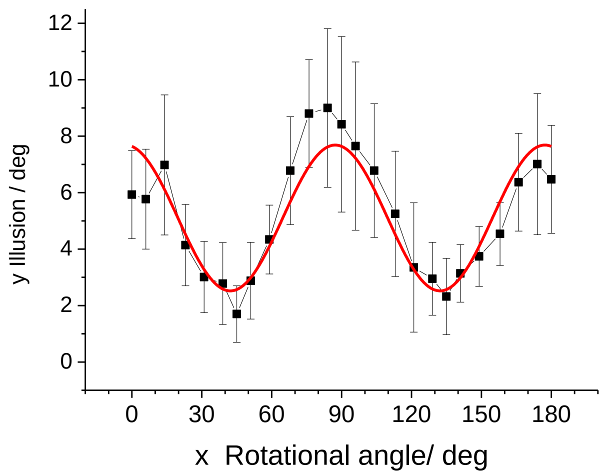

Fig. 11 Fit of a cosine function to the results of an investigation of the Poggendorff illusion. Average of four data sets (Kreiner, 2012).

Function:
y=D+S1*cos(4*(x-S2))

Parameters:
D= 5.10(19)
S1= 2.58(25); S2= -2.75(156)

Chi^2/DoF = 0.86066
R^2 = 0.83212

3. Variants of size constancy

3.1 Guessing the supposed true size

From the data given by Schur (1925) a size constancy parameter of n=0.578(22) has been found for horizontal direction of observation. This means that, when increasing the distance of observation by a factor of four, an object would appear about twice as large as one would expect it from geometrical optics. For vertical direction of observation, n turned out to be considerably smaller [0.319(34)].

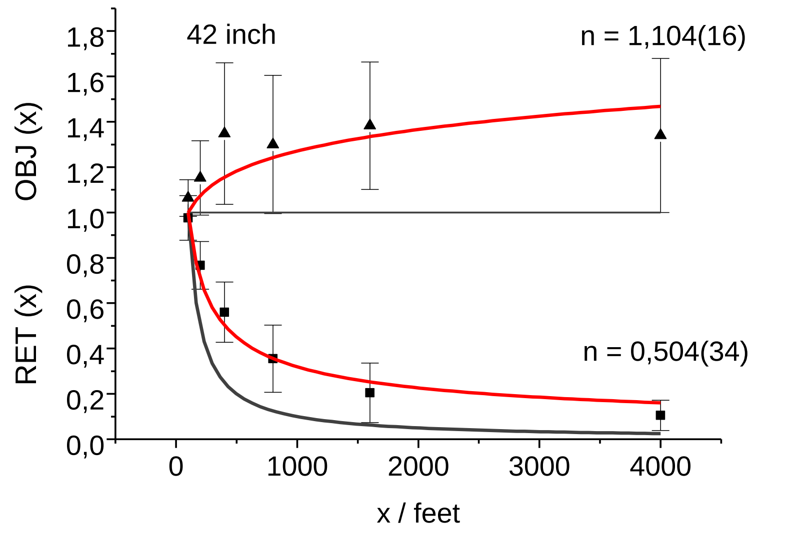

Fig. 12 Experiment by Gilinsky (1955).

Apparent size of an isosceles triangle as a function of the distance of observation, x. RET means the perceived size (lower red curve), OBJ the supposed true size, both as a function of the distance of observation. The true size is overestimated. The black curve refers to the size of the retinal image.

Function:
y=(x/d0)^(n-1)
Results: see figure

Gilinsky (1955) performed a similar experiment with isosceles triangles, achieving a similar size constancy parameter [n=0,504(34)]. In another experiment subjects were asked to indicate the true size of the target. It turned out that it was always overestimated, leading to a size constancy parameter n>1 (Fig. 12).

3.2 Variation of size at constant distance

A size constancy effect is found as well when, instead of the distance of observation, the height of the triangles is varied (Gilinsky, 1955). The function to be fitted has to be slightly modified. The size constancy parameter can be still employed (Kreiner, 2009). The perceived size of an object varying in size (but not in its distance) is $SR(r) \sim (1/\ r_{ret})^{n-1}$, where r_{ret} means the size of the object´s retinal image. Smaller objects appear larger than expected from geometrical optics. Fig. 13 gives the perceived size of isosceles triangles (height: 78, 66, 54, and 42inch) at a distance of 100 feet (left, top), 200, 400, 800, 1600, and 4000 feet. The first value (top, left) means the perceived size of the 78`` triangle observed from a distance of 100 feet. All other values are standardized to this value. The mean size constancy parameter was found to be n= 0,420(27).

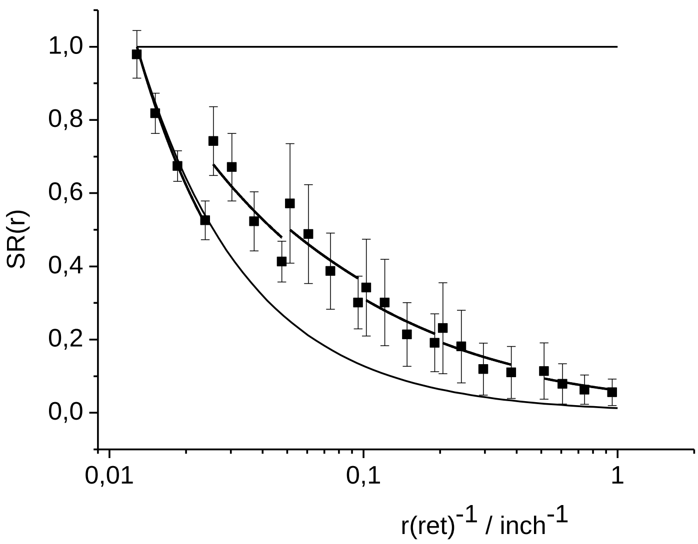

Fig. 13
Relative perceived size of four isosceles triangles of different height watched from the same distance.

Each of the groups corresponds to a certain fixed distance: 100, 200, 400, 800, 1600, and 4000 feet.

The solid grey line gives the size of the retinal image. The first four values (100 feet) show the true size, because the reference triangles used for comparison were positioned at a distance of 100 feet as well. The average size constancy parameter was found to be n= 0,420(27).

3.3 Influence of structural density of the context. Stroke pattern

Size constancy in the sense that the perceived size of a target varies in a way not in proportion to the retinal image can be triggered by context elements of varying size or structure density as well. In experiments of this kind the size of the target, e.g., a straight line, a circle or a square, is kept constant, the observation distance too. However, it is observed that the perceived size of the target depends on certain structural characteristics of its context, eg, its spatial frequency or some other kind of information density. As an example, let us take a horizontal target line, with a regular pattern of parallel vertical strokes as the context elements. Observing just the pattern (without the target line) from some distance will produce a retinal image of certain size. Increasing the distance of observation will reduce the size of the image and, simultaneously, increase the spatial frequency characterizing the pattern. However, a comparable effect will be achieved when reducing the size of the pattern, but keeping the distance constant. Bearing in mind the conceptual model which explains size constancy effects from a reduction of the extent of the visual field in order to improve resolution, it follows that a finer stroke pattern will result in perceptual enlargement and, simultaneously, lead to a perceptional enlargement of the target line, too.

In case the effect is triggered by a texture exhibiting a spatial frequency x, the perceived increase in the target´s size can be expressed as a power function of x, ie,

$$\boxed{y(\text{perc, target}) \sim x^{(n)},}$$

where n, again, is the size constancy parameter. To check this expression, one may set n=0. In this case, as x^(0) = const., a finer structure of the context elements will induce no apparent enlargement of the target. For n=1, on the other hand, the target will appear enlarged in proportion to the spatial frequency, which may be expressed by the number of lines per unit length or by the inverse separation of any sort of structural elements.

In Fig. 14 the perceived length of a red line is plotted versus the structure density of the inducing pattern, consisting of five white vertical lines above black ground. On a DIN A4 plot, the length of the target line was 61mm. The stimuli were projected with a beamer. Inspecting Fig. 14, one finds that the perceived length of the red line is considerably smaller than its true length of 61mm. This is explained from the way how the experiment was performed: The subjects determined the apparent length from comparison with a staple of parallel standard lines. Therefore, each of these lines was imbedded into another kind of

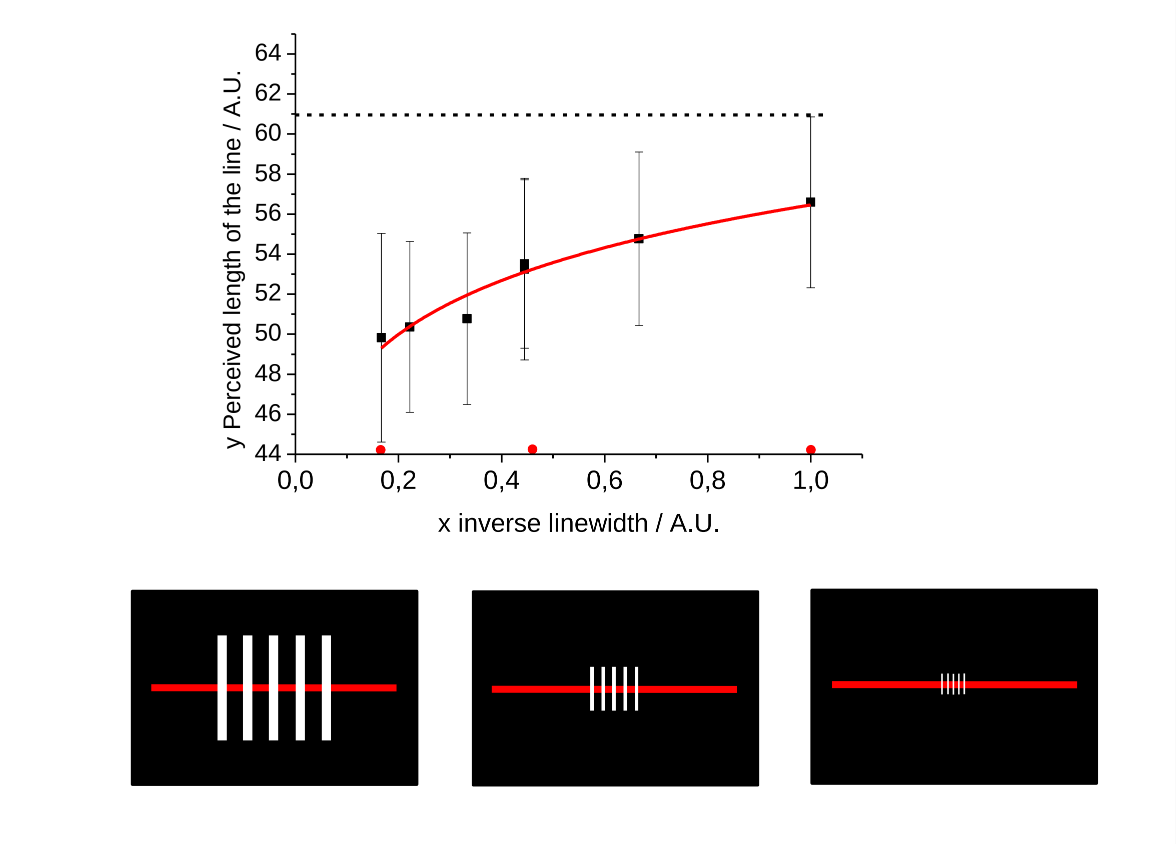

Fig. 14. Perceived length of a red line as a function of the structure density of a contextual pattern (five vertical strokes). The red dots on the abscissa correspond to the stimuli shown below the diagram. The dotted line at 61mm gives to the true length of the target.

Table 2. Data referring to Fig. 14

Target: Horizontal line, length 61mm Inducing pattern: 5 vertical stripes	Function: y=A*x^(+n) Parameters fitted: A= 56.46(45); n= 0.0757(77) Chi^2/DoF= 0.37701 R^2 = 0.95022

contextual structure, leading to some other sort of size constancy effect, too. However, this has no influence on the value of the size constancy parameter n.

4 Compound Illusions

To some illusions several effects seem to contribute. The basic functions described so far may serve as a modular system which allows building up more complicated algebraic expressions. In a typical case, two opposing effects contribute to the illusion, one enhancing and the other one reducing the illusion magnitude. As they usually depend on the independent variable in a different way, the magnitude of the illusion exhibits a maximum for a certain value of x.

4.1 The Checkerboard illusion

Giora and Gori (2011) found that the perceived size of a square depends on the space frequency of the filling texture. This texture showed a square pattern with either (2x2), (4x4), (8x8), (16x16) or (32x32) subparts of equal size. The small squares were filled either in the checkerboard manner (black and white), or randomly with black, grey and white squares, arranged in an irregular way (Fig. 15). Fig. 16 gives data of the checkerboard arrangement. There, the relative perceived increase in the length of one side (square root of the relative increase in size) is plotted versus the number of microelements x along one edge. The

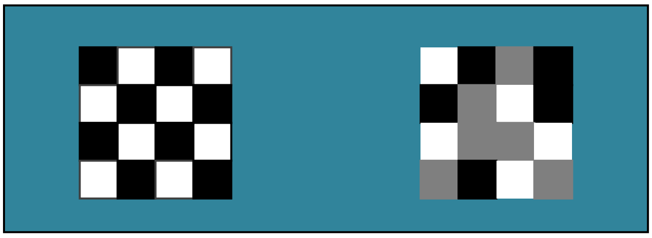

Fig. 15
Examples of square patterns presented in the experiments of Giora and Gori (2011).

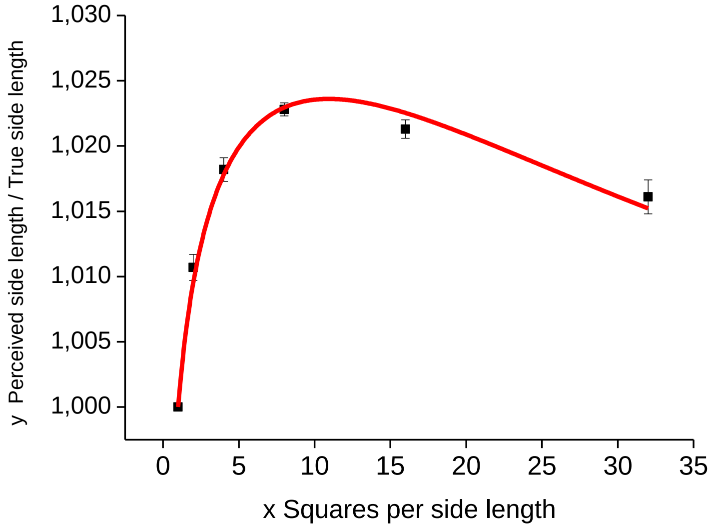

Fig. 16 Perceived size of a square as a function of the space frequency of the texture. Checkerboard arrangement Data: Giora et al. (2011).

Function:
y= x^(n·exp(-B·x))

Parameters:
n= 0.0148(6)
B= 0.0382(26)

Chi^2/DoF= 9.4652E-7
R^2 = 0.98935

maximum indicates that there are at least two interacting and opposing effects involved. The visual system, so the size constancy hypothesis, will zoom into structured texture in order to improve resolution, leading to perceived enlargement of the object´s image. However, there is a limit to the resolving power of the eye, where further reduction of the visual field would not produce any more details. In addition, in case of a uniform pattern better resolution (and sacrificing attentional angle) would not produce more information. To account for this, the size constancy parameter is assumed to decrease exponentially with the space

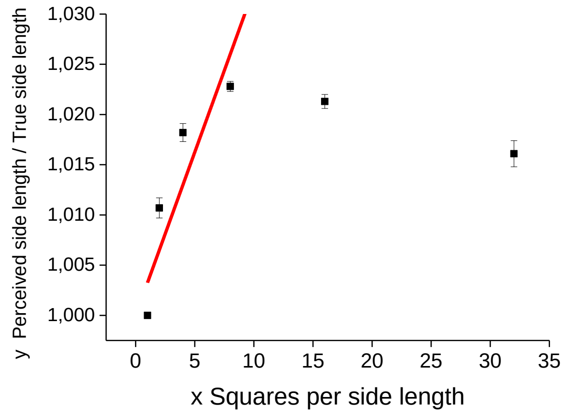

Fig. 16a

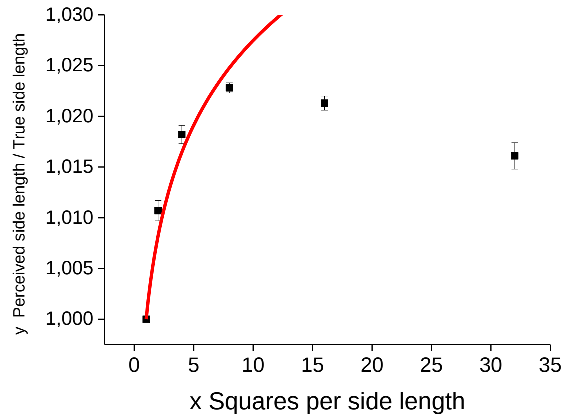

Fig. 16b

Linear fit: y= 1+A*x; A= 0.00325(51)
Chi^2/DoF= 0.00002; R^2= 0.77978

Power function: y= x^(n) n= 0.01177(79)
Chi^2/DoF= 4.4202E-6; R^2= 0.9554

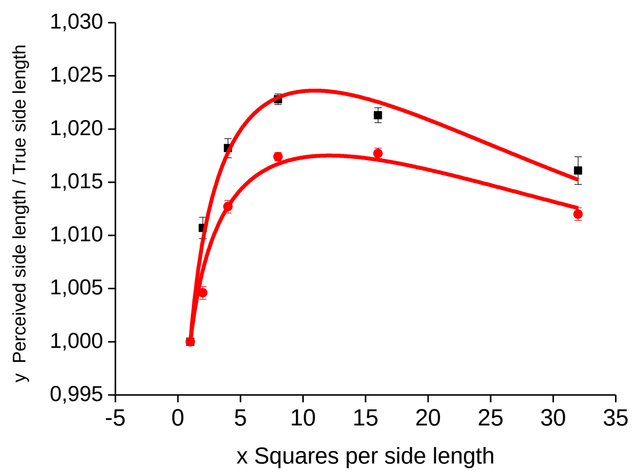

Fig. 17

Function: y=x^(n*exp(-B*x))

Upper curve:
Checkerboard arrangement
n = 0.0148(6) B=0.038(26)

Lower curve:
Random arrangement
n = 0.01039(71) B=0.0331(41)

frequency. The function employed is $\boxed{y=A*x^{(n*exp(-B*x))}}$.

In Fig. 16 only the first four values have been used for fitting (linear and power function). Fig 17 gives the fit with the complete function, for the regular as well as for random arrangement.

4.2 Variants of the Baldwin illusion

4.2.1 Classic Baldwin illusion

In its classic version (Baldwin, 1895) a straight horizontal line serves as a target, two squares are attached to its ends (Fig. 20). With increasing size of the squares, the length of the target first appears to increase slightly, but then, after a smooth maximum, it drops to values considerably below the perceived starting length. The increase and the decrease are usually ascribed to assimilation and contrast effects, respectively. Here it is interpreted as due to averaging and size constancy (Kreiner, 2004). Context elements, their shape, their size and their position, exert an influence on the perceived midpoint or the length of a line (Baldwin, 1895). Due to [Brigell, Uhlarik, and Goldhorn (1977); Wilson and Pressey (1988)] the perceived length of a horizontal line extending between two squares first increases slightly as a function of the framing ratio, followed by a smooth maximum, and then decreases steeply, finally approaching an asymptotic value (Figs. 18, 19; data from Brigell et al.).

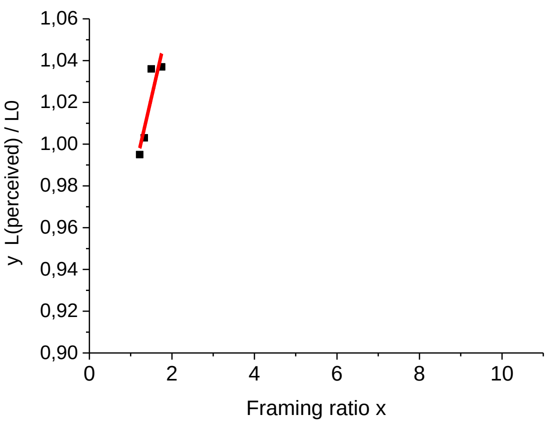

y=D+A*(x-1)   D= 0.979(14)   A= 0.086(29)

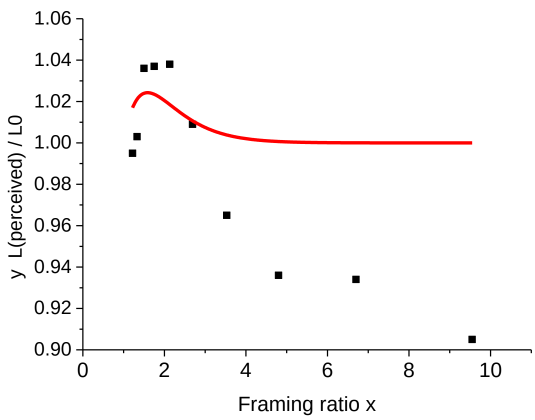

y= 1+A*(x-1)*exp(-B*L0*abs((x-1)))
A= 0.11(23) B= 0.017(26) L0=100 (fixed)

Fig. 18
Left: Linear function, fitted to first values only.
Right: Exponential decay function is added

The experimental values plotted in Fig. 19 give the perceived length of the target line divided by its true length L0 (=100). The function employed for fitting is built up in the following way: The 1 within the first bracket corresponds to L0. Then, to first order of approximation, the deviation from L0 is given by the expression A*(x-1), describing the averaging effect, where averaging means that the apparent length of the target line increases with the size of the boxes. A is a parameter to be fitted, (x-1) is equal to the width of the two boxes divided by L0. This expression is zero for x=1, where the boxes are yet infinitely small. Further, it is assumed that averaging fades away gradually, which is approximated by the exponential decay function exp(-B*L0*abs(x-1)). Finally, size constancy is taken into account by the power function, where (L0*x) means the full extension of the stimulus and n, again, is the size constancy parameter. For large x the exponential decay term seems to play a dominant role.

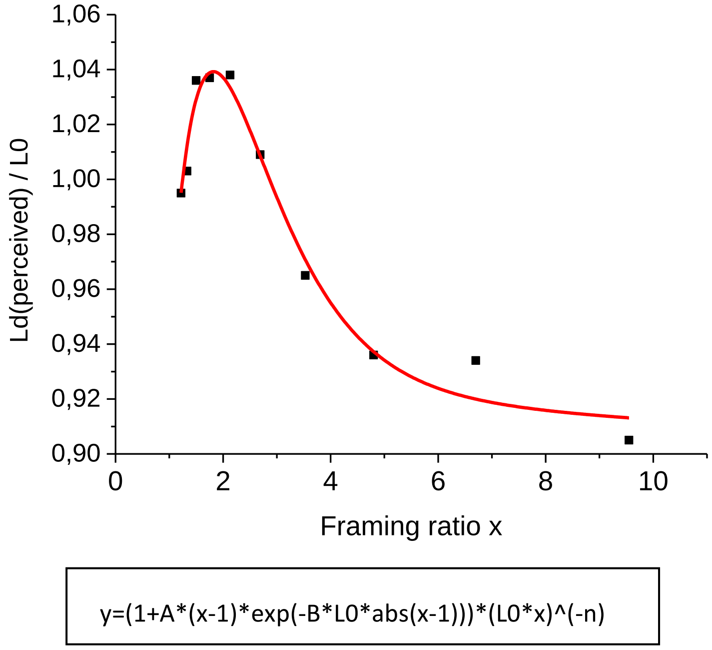

Fig. 19 Effect of adding a power function with the size constancy parameter in its exponent. Data: Brigell et al.

A= 0.355(26)
B= 0.01147(67)
L0= 100 (fixed)
n= 0.01327(84)

Chi^2/DoF= 0.00006
R^2 = 0.97828

Examples of stimuli are given in Fig. 20. With increasing framing ratio, the stimulus becomes larger. In contrast to the stimuli with a gap described in chapter 4.2.2, the three elements always remain a geometric unit. This, in addition to the fact that the variation of the total size of the stimulus extends over nearly one order of magnitude, might be a major reason why size constancy plays a dominant role.

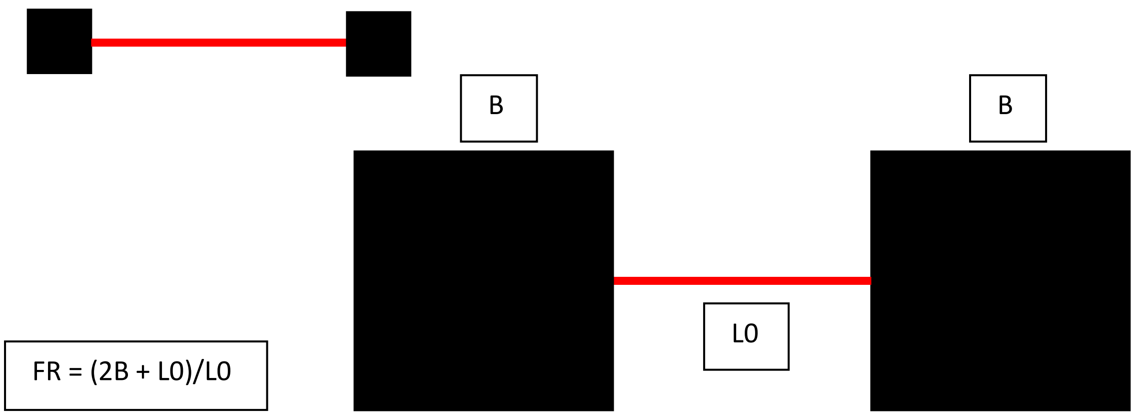

Fig. 20 Classic Baldwin illusion, examples of stimuli. In contrast to the stimulus described in chapter 4.2.2, the context elements are always attached to the ends of the target. They just vary in size.

4.2.2 Baldwin with gaps

The following variant of the Baldwin (1895) illusion is one of the rare cases where the magnitude of the illusion exhibits a singularity concerning its dependence on the independent variable. In this experiment full black squares of constant size are placed symmetrically at various positions along the axis of the target line, either within the length of the line or at some distance beyond its ends, leaving a gap. It is observed that the smooth maximum turns into a sharp peak (Figs. 22 and 23). This peak is mainly ascribed to averaging which occurs as long as the context elements are attached to the ends of the line. Averaging decreases rapidly with increasing gaps. It is assumed this is because the stimulus then does not present a uniform geometric element any more. Concerning the magnitude of the effect, the orientation of the stimulus plays an important role, too.

The framing ratio was varied between 0.67 and 3.08 (Kreiner, 2011, 2012). In Figs. 22 and 23 the experimental values are plotted versus the framing ratio x. For the fitting procedure the function

$$y= D+A*x+A2*exp(-B*(abs((3*x - 5)/2)))$$

was chosen. The expression (3*x-5) follows from the geometry of the stimulus. With the squares attached to the ends of the target line, the framing ratio is 5/3. The maximum illusion occurs around x=1.67 where 3x-5 = 0. Tilting the stimulus by 30, 45, and 90 degrees enhances the illusion, but not quite in proportion to the angle of inclination.

Fig. 21 Examples of stimuli presented.

The framing ratio is defined as $FR=(2S + 2d + L_0)/L_0$

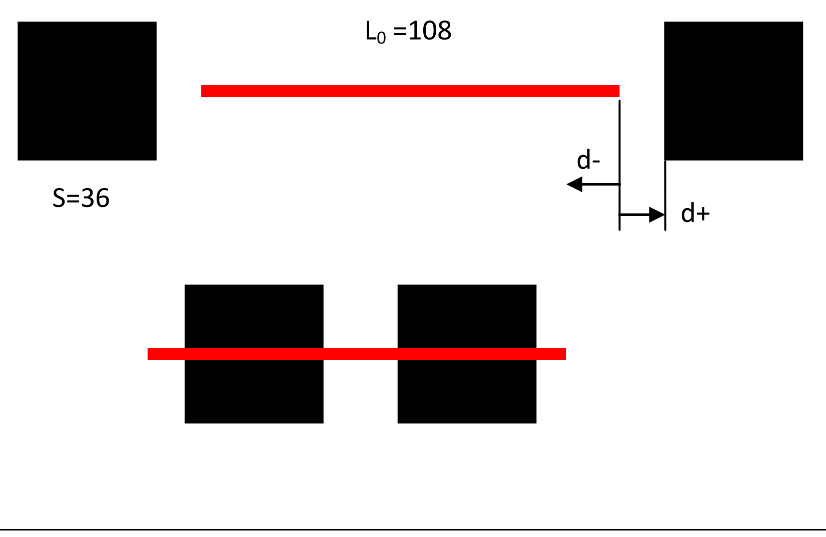

Figs. 22 and 23 give the results for the horizontal and vertical orientation of the stimulus, respectively (Kreiner, 2011). The maximum occurs when the boxes are attached to the ends of the target line, forming a structural unity (d=0). In this case, averaging appears to be most efficient. The sharp decrease towards higher and lower values of the framing ratio is interpreted as due to a loss of the geometric context as soon as the line is more and more recognized as an element of its own. In addition, a slight overall increase of the values in proportion to the framing ratio is observed (Figs. 22b, 23b).

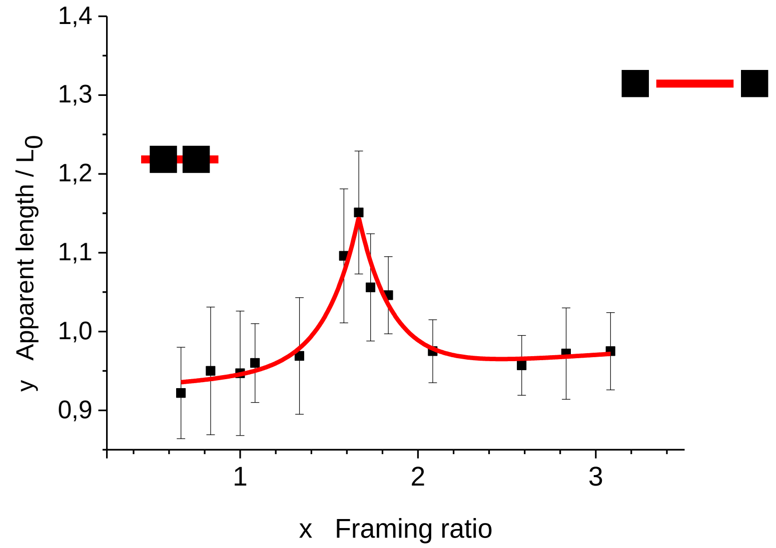

y=D+A*x+A2*exp(-B* (abs((3*x - 5)/2)))

Fig. 22 a Perceived length of the red target line as a function of the framing ratio. The sharp peak occurs when the squares are attached to the ends of the target line.
Target: Horizontal orientation

D= 0.924(13)
A= 0.0153(61)
A2= 0.195(14)
B= 3.49(67)
Chi^2/DoF= 0.00025
R^2= 0.95838

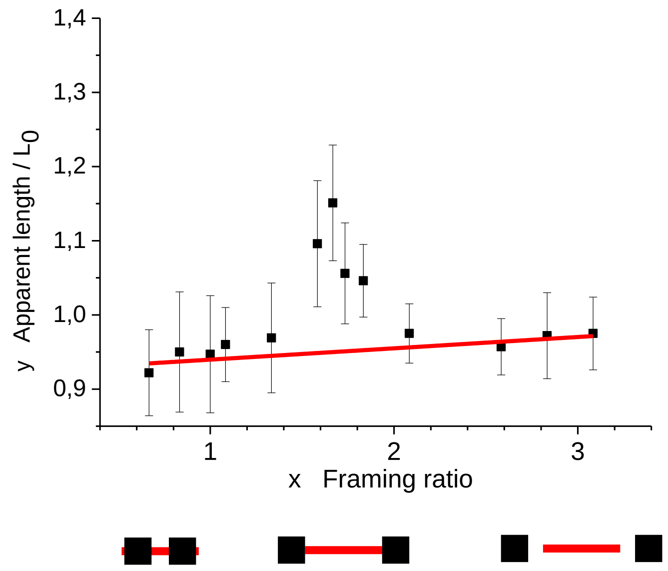

Fig. 22 b

Target: Horizontal orientation

Function:
Left: y = D +A*x

D and A from Fig. 19a.

A quite similar observation is made on the dumbbell illusion, where the squares are replaced by full circles. In this case, the exponential decay on either side of the maximum seems to be less steep (Kreiner, 2009, 2012).

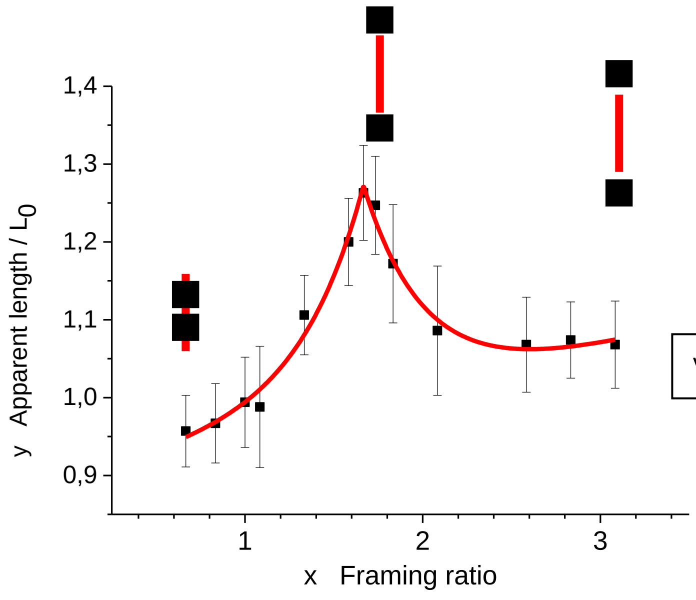

Fig. 23a Perceived length of the target line for vertical orientation of the stimulus

Function:

y= D+A*x+A2*exp(-B*(abs((3*x - 5)/2)))

A= 0.0566(63)
A2= 0.283(13)
B= 1.89(29)

Chi^2/DoF= 0.00023
R^2 = 0.9835

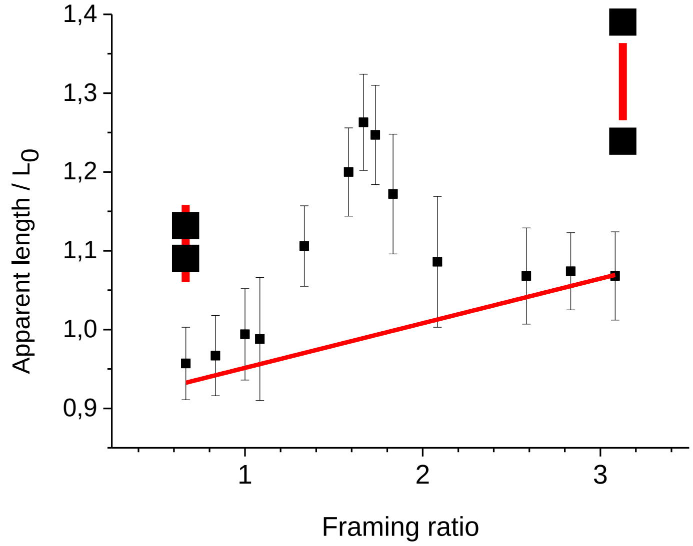

Fig. 23b

Target: Vertical orientation

Function:
y = D +A*x

D and A from Fig. 20a.

4.3 The Müller-Lyer illusion

Since Müller-Lyer (1889) first published this illusion it has been investigated by several authors (e.g., Yanagisawa, 1939; Fellows, 1967; Pressey, Di Lollo, and Tait, 1977; Predebon, 1994). The apparent length of the shaft depends primarily on the geometric properties of the wings or fins (their length, the angle they subtend, whether the fins are ingoing or outgoing), and on the framing ratio (Figs. 24 to 26). Depending on whether the range spanned by the context elements is slightly larger or smaller than the length of the target line, it is perceived as being longer or shorter than its true length, respectively. This phenomenon, usually called assimilation, is explained by a theory of Pressey (1971) as an averaging effect. It states that the apparent length of the line is averaged with the contextual magnitudes.

In the investigations discussed next, gaps were left between the shaft and the ingoing wings (Fig. 26), their size being varied from zero to about half the length of the shaft. It was found that the perceived length of the shaft as a function of the framing ratio first increases (reversed Müller-Lyer effect; Pressey et al., 1977), but then decreases again. The smooth maximum (Fig. 25) occurs at a framing ratio where the wings are positioned near the ends of the shaft, but still partly overlap with its ends. In contrast to this observation, in case of outgoing wings (Fig. 27) the apparent length of the shaft decreases continuously from zero gap on (Predebon, 1994; Fig. 28). The question arises what the apparent length would be when the outgoing fins were positioned at even shorter distance, i.e., *within* the length of the shaft (Fig. 27, bottom) and whether the shape of the curve would be similar or significantly different from the one describing ingoing wings.

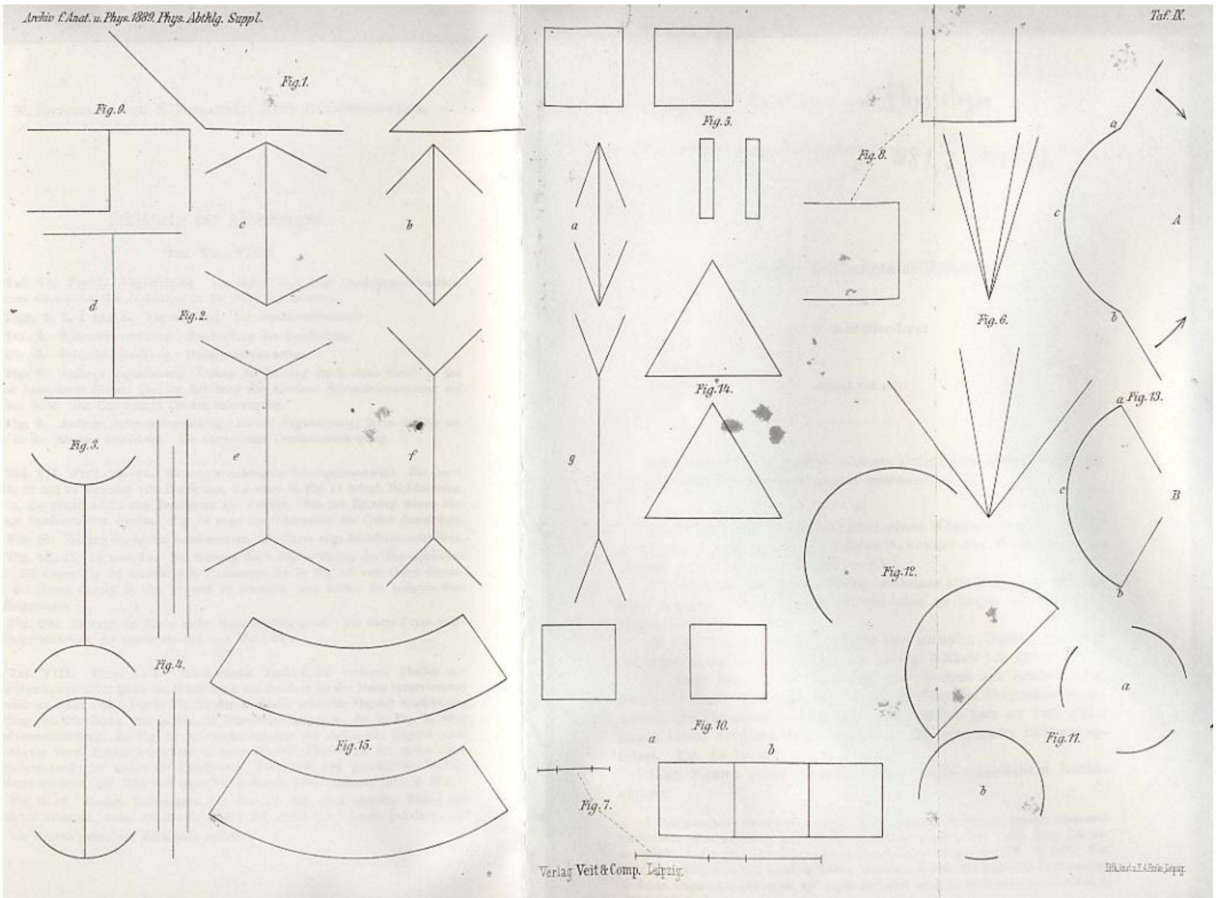

Fig. 24. Drawing by Müller-Lyer, published in 1889 in the *Archiv für Anatomie und Physiologie.*

4.3.1 Ingoing wings

The data in Fig. 25 have been published by Pressey et al. (1977). Horizontally, the framing ratio FR is plotted (defined in Fig. 26). On the vertical axis the perceived length of the shaft in relation to its true length L_0 is given. For fitting, the function

$$L(perceived)/L_0 = D + A\cdot(x-1)\cdot \exp[-B\cdot abs(x-1)]$$

has been employed. (x-1) corresponds to twice the gap size, so the curve shows the magnitude of the illusion as a function of the gap size, too. The illusion had been measured for six angles of the (ingoing) fins. For the plot, the experimental results of each two of them had been combined (30^0+60^0, 90^0+120^0, 150^0+180^0).

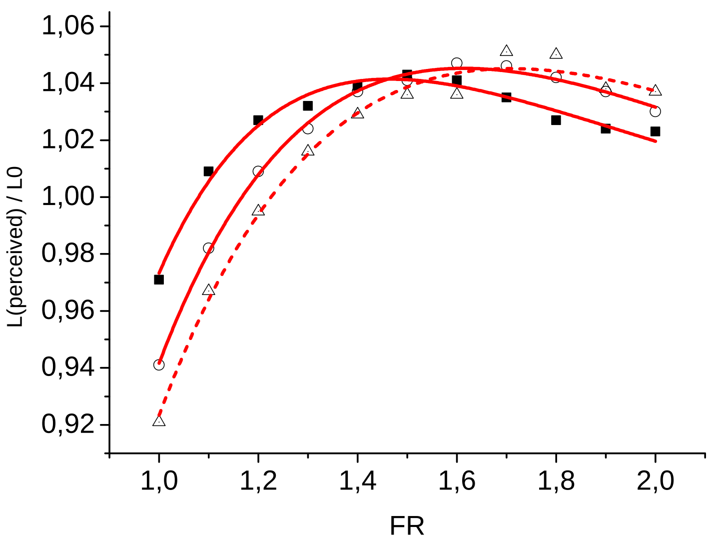

Fig. 25 Apparent length of the shaft plotted against the framing ratio. Ingoing wings.
Function:
y = D+A·(x-1) · exp[-B·abs(x-1)]

DEL= 0.9733(28)
A= 0.399(26) ■
B= 2.153(74)

DEL_2= 0.9417(28)
A_2= 0.459(23) ○
B_2= 1.629(49)

DEL_3= 0.9234(28)
A_3= 0.467(21) △
B_3= 1.411(44)

Chi^2/DoF= 0.00001
R^2 = 0.99193

Fig. 26 α:

150^0 + 180^0	■
90^0 + 120^0	○
30^0 + 60^0	△

Ingoing wings

FR = S/L0

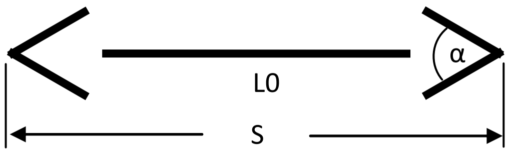

4.3.2 Outgoing wings

Outgoing wings produce a noticeably different curve (Kreiner, 2012). The length of one wing is 0.41·L0, with L0 again being the target length. The horizontal extension of one arrowhead is 0.375·L0. There is a sharp peak at x=1.75, occurring at the maximum value where there ist still overlap, ie, where the wings are just attached to the ends of the target line [(2·0375·L0 + L0)/L0 =1.75)]. In addition, there is a general trend of the magnitude of the illusion to decrease with increasing x, corresponding to the negative value of the parameter A (Fig. 28).

Fig. 27 Target, outgoing wings

α = 50 degrees

FR = S/L0

Framing ratio < 1.0

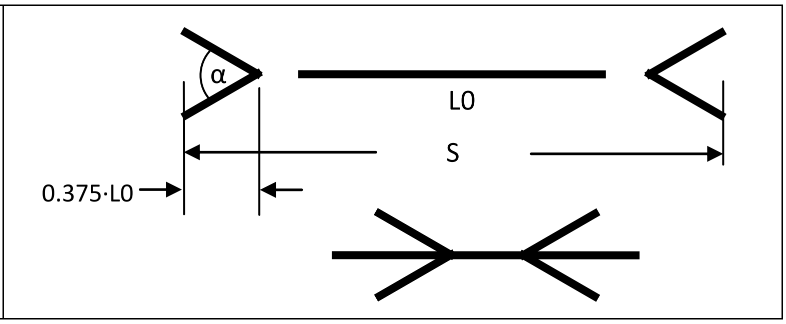

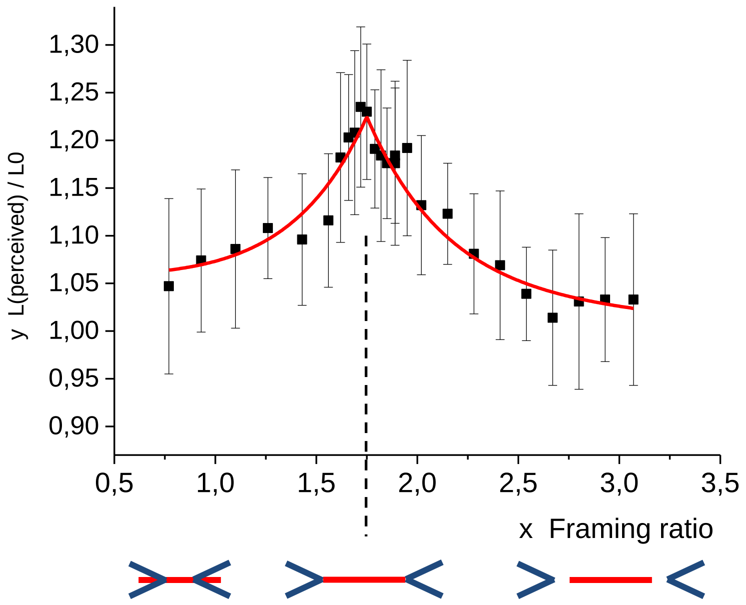

Fig. 28 The Müller-Lyer illusion on a shaft with outgoing wings.

Function:
y = D+A*(x-1.75) + A2*exp(-B*abs(x-1.75))

Parameters fitted:
D= 1.035(18)
A= – 0.0135(82)
A2= 0.190(16)
B= 2.55(63)

4.4 Delboeuf illusion

Among the illusions showing the effects of assimilation and contrast, the Delboeuf (1892) illusion is unique in two respects: The target and the inducing context element are identical in shape, and, although there is a gap between the target and the inducing circle, both seem to stay a unit because they are concentric, giving the impression of a ring. The term contrast usually indicates that, in case the context elements extend over a range considerably larger than the target, the target size will become apparently smaller than it is perceived without any context. Again, assimilation will be replaced by the term *averaging* and contrast by *size constancy effect*. In the Delboeuf illusion (Figs. 29, 30, 31), the size constancy effect on a circular line of constant diameter (the target) can be expressed by a power function of the framing ratio, y(perc, target) ~ x^(-n). In case there is no influence of the inducing circle on the target (n=0), the perceived size of the target will stay constant.

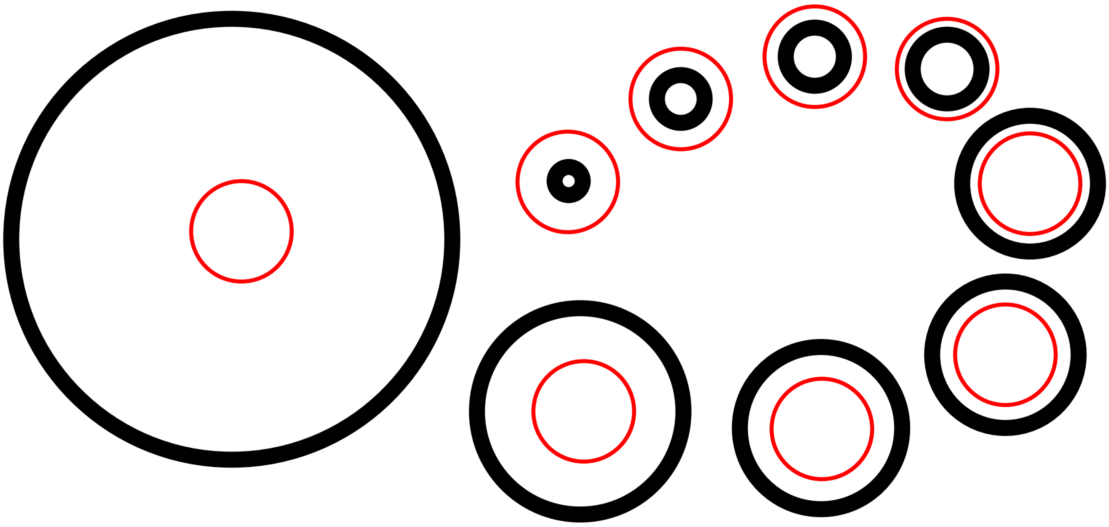

Fig. 29 Example of the Delboeuf illusion. All the red circles are of identical size.

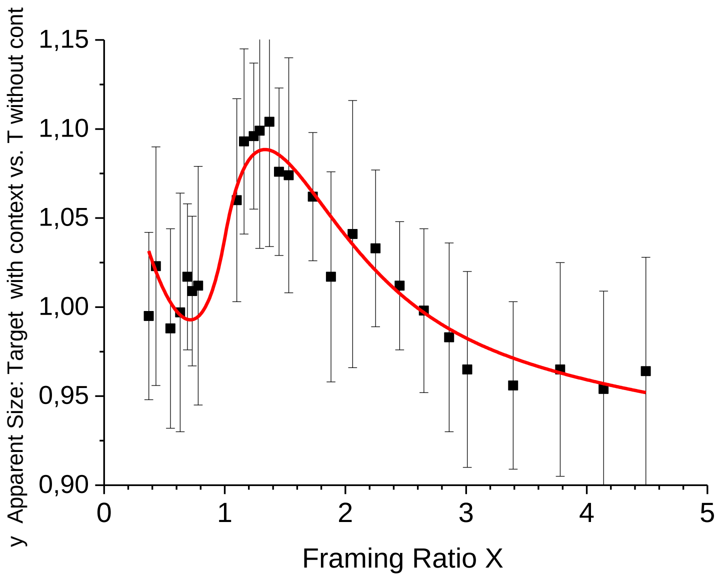

Function fitted:

y= (1-A*(1-x)*exp(-B *abs(1-x)))*C2*x^(-n)

Parameters obtained:

A= 0.422(57)
B= 2.29(31)
C2= 1.0387(37)
n = 0.0584(64)

Chi^2/DoF= 0.00026
R^2 = 0.89937

Fig. 30 Delboeuf illusion. Apparent size of the target circle (normalized to d_0, its apparent size without context) as a function of the framing ratio. For framing ratios just below and above 1, averaging leads to an apparent decrease or increase of the target circle, respectively. For very large x-values the size constancy effect causes apparent shrinking of the stimulus.

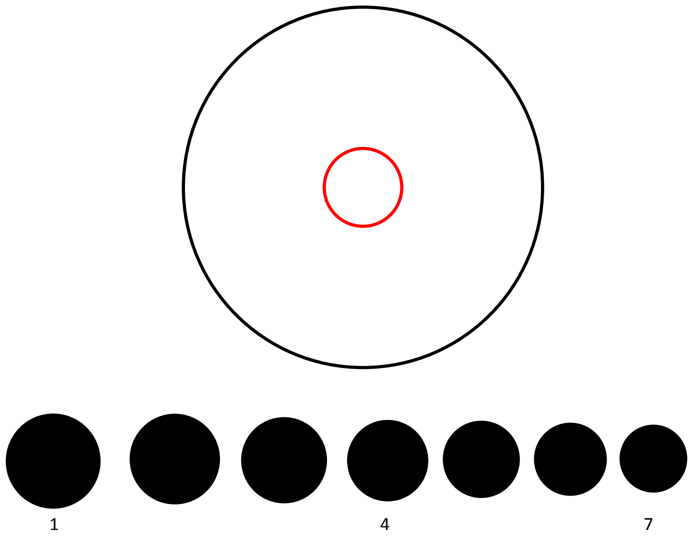

Fig. 31

One of the transparencies presented. Framing ratio is 4.49 (ratio of the outer diameters). Standard circle # 4 matches the red target.

4.5 Zöllner illusion

There are several variants of the illusion first described by Zöllner (1860). In general, a field of oblique parallel lines makes a single horizontal or vertical line to appear tilted. Wallace and Crampin (1969) investigated the effect of background density of parallel lines on the Zöllner (1860) illusion. In the example given here the magnitude of the illusion has been investigated on the parallel sides of a rhombus (which are close to the vertical) as a function of the rotational angle of the inducing field (Fig. 32). The orientation of the background field was varied in steps from 4^0 (with respect to the vertical) to 45^0. A set of five diamonds was given for comparison. The results are plotted in Fig. 33. They give the perceived deviation of the parallel side from the vertical.

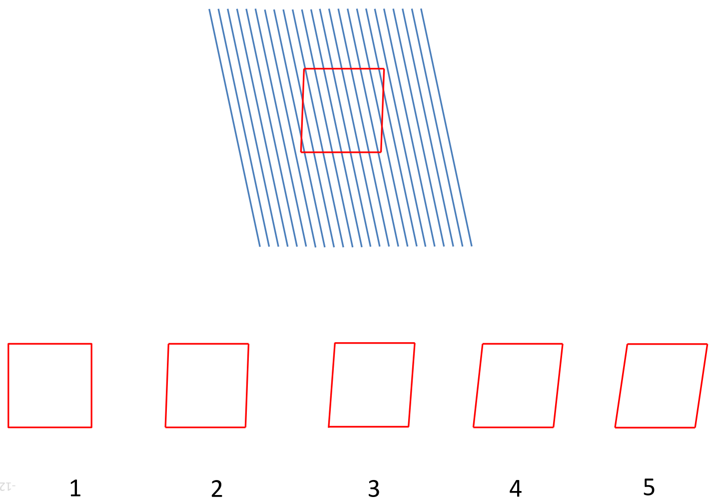

Fig. 32 the parallel sides of a rhombus appear to be inclined even more.

Target:

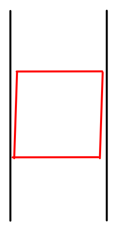

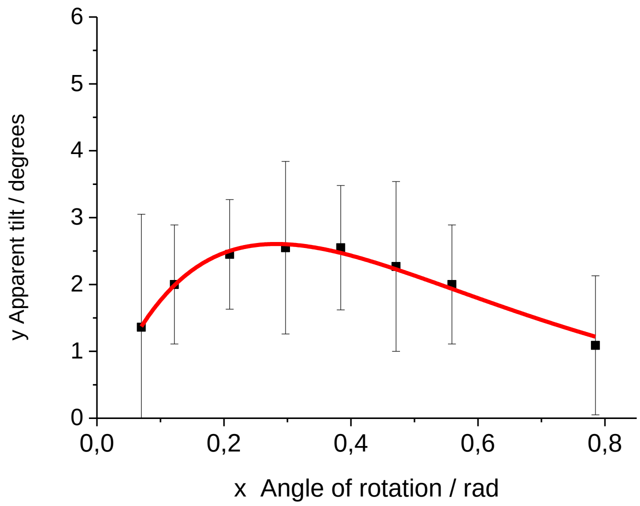

Fig. 33 Apparent inclination of the nearly vertical sides of a rhombus as a function of the angle of rotation of the inducing field. Maximum inclination is 2.6^0, when the field is rotated by 16^0.

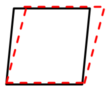

Function:
y=A·x·exp(-B·x)

Parameters:
A= 25.11(72)
B= 3.545(76)

It is assumed that, at small intersect angles, the perceived additional tilt of the parallel sides is in proportion to the angle of rotation of the inducing field. This influence is supposed to decrease exponentially with increasing angle of rotation. This is expressed by the function y=A·x·exp(-B·x), where x means the angle of counter clockwise rotation.

4.6 Poggendorff illusion with context elements

An oblique line is partly occluded by a vertical bar. The thought continuation of one of the protruding segments appears to miss the other one. The questions is whether this apparent shift is due to a perceived vertical shift or a tilt of the segments or whether just the thought

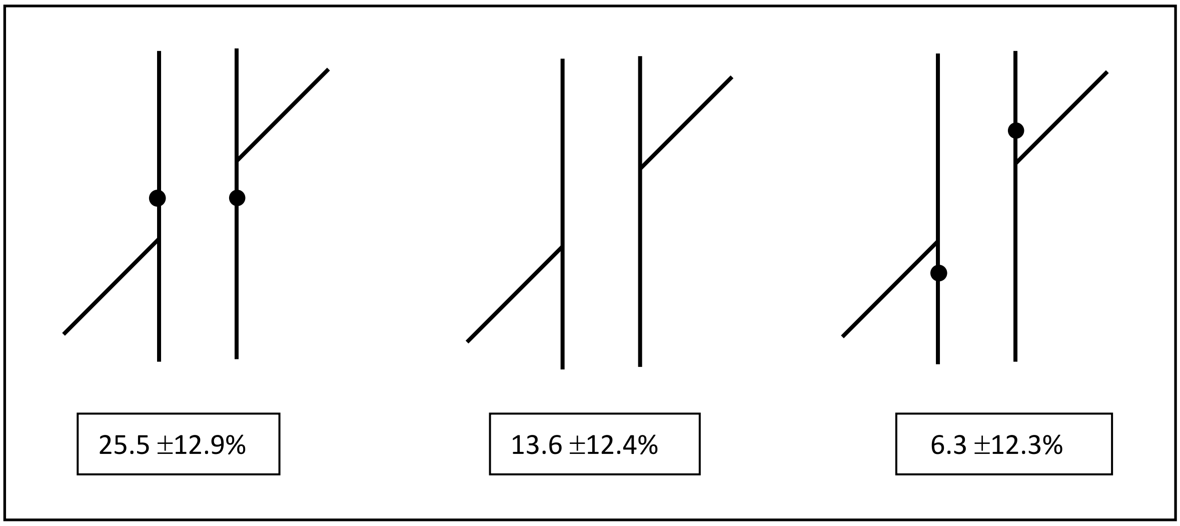

Fig. 34 Classic Poggendorff illusion (centre): The protruding ends of the crossing line appear to be vertically offset. Left: The magnitude of the illusion is enhanced, when the dots are positioned at the same height halfway between the merging points, but reduced, when they are just above and below them (right). The apparent vertical shift is given in relation to the width of the occluding bar.

extension of a segment across the occluding bar deviates from the true orientation of the target line. This has been studied extensively [eg, Obonai, 1931; Weintraub and Krantz, 1971; Weintraub, Krantz, and Olson, 1980); Wenderoth et al., 1978)]. In the example given here the influence of context elements is investigated (Kreiner, 2012). Two dots are positioned symmetrically right on the edges of the occluding bar and shifted vertically. The maximum illusion is observed when the dots are aligned horizontally, halfway between the merging points (Fig. 34). In the experiment, stimuli were shown with the dots in different positions along the edges, always opposite to each other with respect to the centre of symmetry. When coinciding with the merging points (x=0), the illusion corresponds to the classic variant. As the experiments of Wenderoth et al. (1978) have shown, the thought extension of an oblique line is turned slightly towards the horizontal when it is stopped by an inducing vertical line. Here, the dots seem to act in a twofold way, depending on their position: When placed halfway between the merging points, they strongly enhance the apparent shift. In addition, reduction or enhancement is observed depending on whether the dots are positioned either above and below (Fig 35, left) or within the merging points (right). The effect is quite pronounced for small values of the x coordinate and fades away for large x. To first order this is approximated by a term ~x*exp(-B*(abs(x))):

$$y = D-A*x*exp(-B*(abs(x)))$$

Fig. 36 gives the fit.

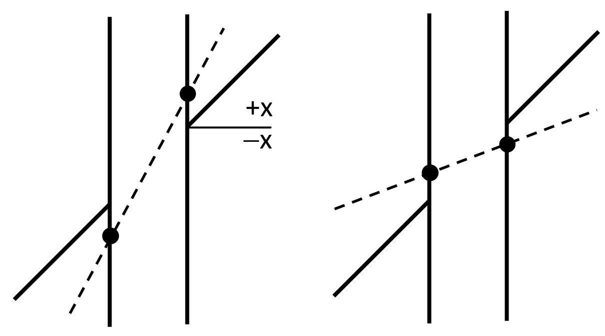

Fig. 35

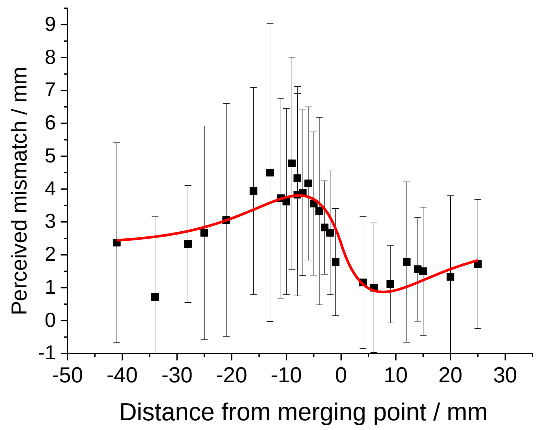

Fig. 36 Poggendorff illusion as a function of the position of dots on the vertical bars.

Function: y = D-A*x*exp(-B*(abs(x)))

Parameters:
D= 2.34(12)
A= 0.52(12)
B= 0.130(22)

Horizontal arrangement of the dots seems to rotate the thought extension of the segments towards the horizontal, too. This effect fades away rapidly with the dots being shifted upwards and downwards. To take this into account, the function y=exp(-B2·abs(x+8)) was employed (Fig. 37).

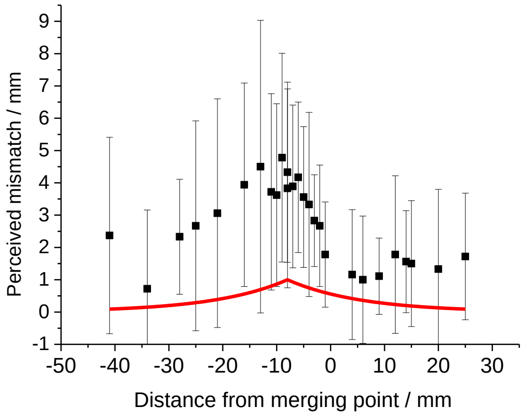

Fig. 37 Effect induced by horizontal orientation of the dots.

Function: y=exp(-B2·abs(x+8))

Parameter: B2= 0.073(19)
(taken from the fit of the complete function, below)

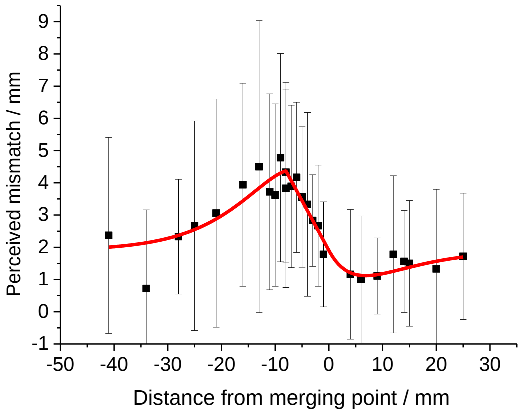

Fig. 38 Fitting of the complete function

Function:
y = D – A*x*exp(-B*(abs(x)))*
exp(–B2*abs(x+8))

D= 1.90(13)
A= 0.553(93)
B= 0.073(21)
B2= 0.073(19)

Chi^2/DoF= 0.20728
R^2 = 0.87778

The complete function (Fig. 38) fitted is

y = D – A*x*exp(-B*(abs(x)))*exp(–B2·abs(x+8)).

4.7 Split circle illusion

Dividing a circle asymmetrically by a vertical bar causes the two segments appear as if they belonged to circles of different size (Fig 39). The size of the smaller segment is underestimated and its relative apparent size further decreases with increasing true size of the large segment. Rotating the stimulus modulates the magnitude of the illusion. The illusion, again, is ascribed to a size constancy effect, similar to the Delboeuf illusion, where the target

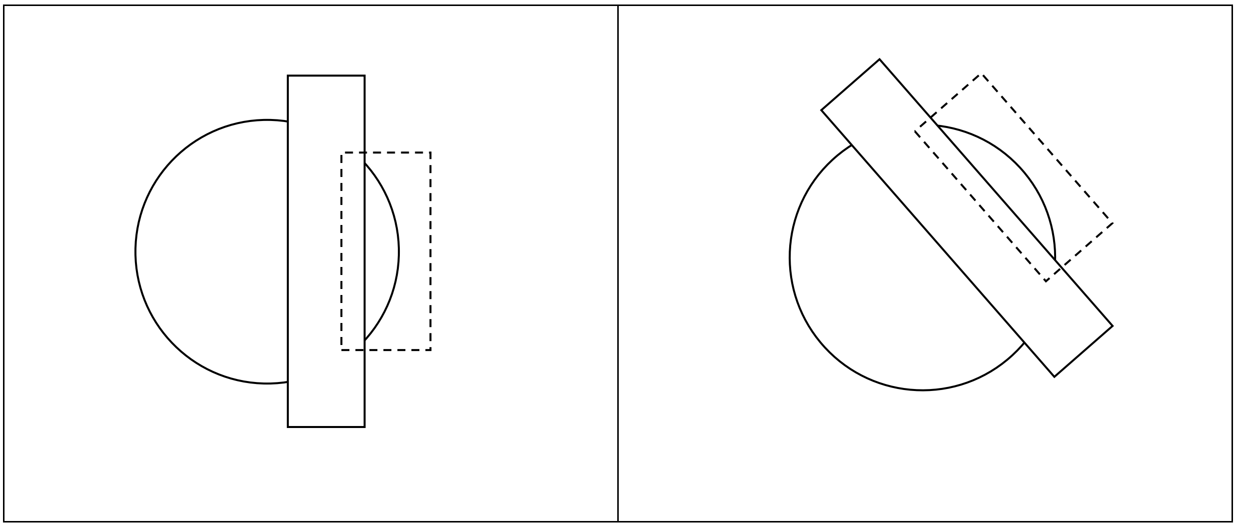

Fig. 39 The size of the small segment is underestimated. The illusion depends on the size of the larger segment as well as on the angle of rotation.

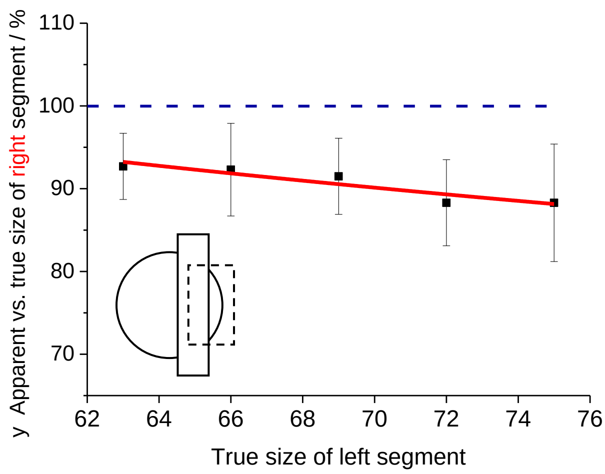

Fig. 40 Apparent size of the small segment in relation to the large one. The size of the smaller segment is underestimated and its relative apparent size decreases with increasing true size of the large segment (size constancy effect).

Function:
y(x) = C2*x^(-n)

Parameters:
C2= 354(109)
n= 0.32(7)

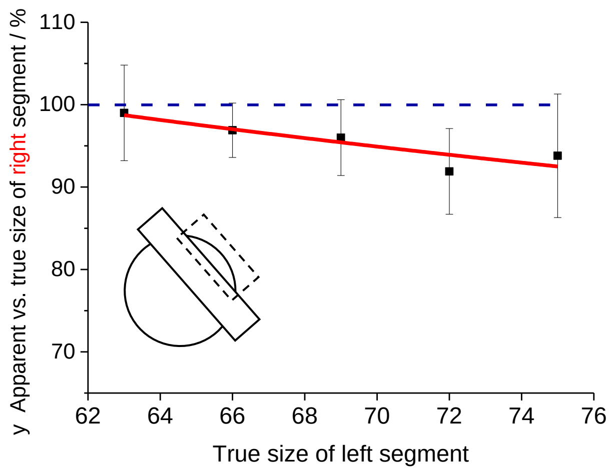

Fig. 41 With the bar tilted by 45^0, the size of the smaller segment is still underestimated, but to a less degree. Again, its relative apparent size decreases with increasing true size of the large segment.

Function:
y(x) = C2*x^(-n)

Parameters:
C2= 192(80)
n= 0.37(11)

circle perceptually shrinks when the context circle gets large compared to the target. For this reason the function y= C2·x^(-n) has been chosen for the fitting procedure, where x means the true size of the left segment (Figs 40 and 41). The same function is part of the algebraic expression in chapter 4.4 (Delboeuf). The fact that the angle of rotation has an influence on the perceived size of the target segment is ascribed to the effect leading to the Poggendorff illusion, too: With the bar in vertical position the thought continuation of the small segment appears to be bent slightly towards the horizontal. Therefore, in comparison to the large segment, the small one appears to be even more reduced in size.

4.8 Oppel-Kundt

The experiments performed by Spiegel (1937) were carried out in the dark. Slits were cut into black cardboard and illuminated from the back (Fig. 1). The distance *cd* between the

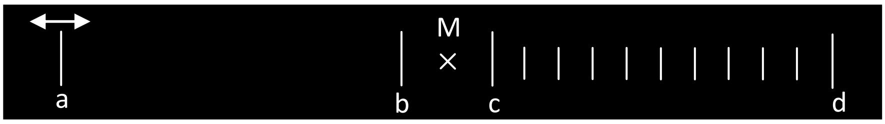

Fig. 42 The distance between the long slits on the left (*ab*) appears to be shorter than on the right (*cd*).

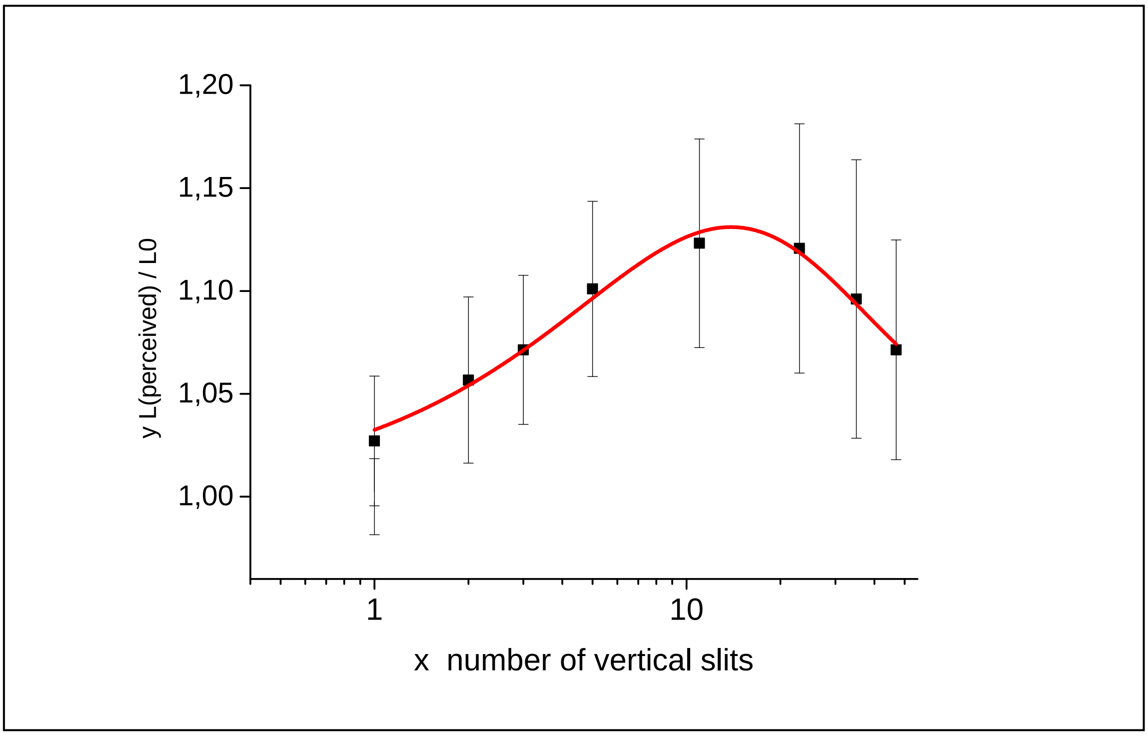

Fig. 43. Perceived length of a distance of horizontal extent (400 mm) as a function of the number of slits. The increase at low x is interpreted as due to the attempt of the visual system to improve resolution (size constancy effect) while the decrease at high x indicates that the filling structure is gradually regarded as a uniform pattern. Distance of observation was 2.7 m.

long slits was fixed in length. It was filled successively with up to x=47 vertical short slits. In the basic experiments they were equally spaced. The position of the slit *a* was variable. The subjects compared the two distances (*cd* vs. *ab*) and indicated as soon as they judged them to be equal.

The increase at low x is interpreted as due to the attempt of the visual system to improve resolution (size constancy effect). In its extreme, a continuous row of elements will merge into a bright line without any structure. For this reason, n is assumed to decrease exponentially, leading to the function

$$\boxed{y= 1+A\cdot x^{[n\cdot \exp(-B\cdot x)]}}$$

with the parameters A=0.0325(22), n=0.775(0,047), and B=0.0274(13).

6. Conclusion

From conceptual models algebraic functions are derived and fitted to the experimental results obtained from investigations on several classic geometric visual illusions and some of their variants. Occasionally, only one of the so called basic functions is needed, in other cases combinations of basic functions are employed. Examples indicate that a fairly low number of algebraic functions is needed to approximate the experimental results of several geometrical visual illusions well within their error limits.

Citations

Baldwin, JM (1895). The effect of size-contrast upon judgments of position in the retinal field. *Psychol. Rev., 2,* 244-259.

Brigell, M, Uhlarik, J, and Goldhorn, P (1977). Contextual influence on judgements of linear extent. *Journal of Experimental Psychology: Human Perception and Performance, 3*, 1977, 105-118.

Coren, S, Girgus, J, Erlichman, H, and Hakstian, AR (1976). An empirical taxonomy of visual illusion. *Perception & Psychophysics,* 20, 129-137.

Delboeuf, J LR (1892). Sur une nouvelle illusion d'optique. *Academie Royale des Sciences, des Lettres et des Beaux Arts de Belgique. Bulletins de l´Academie Royal de Belgique, 24,* 545-558.

Fellows, BJ (1967). Reversal of the Müller-Lyer illusion with changes in the length of the inter-fins line. *Quarterly Journal of Experimental Psychology,* 19, 208-214.

Fraser, J. (1908). A new illusion of visual direction. *British Journal of Psychology, 2*, 307-3290.

Gilinsky, A S (1955). The Effect of Attidude upon the perception of size. *The American Journal of Psychology,* 68, 173-192.

Giora, E and Gori, S (2010). The perceptual expansion of a filled area depends on textural characteristics. *Vision Research* 50, 2466-2475.

Gregory, R.L. (1977). Vision with isoluminant color contrast: 1. A projection technique and observations. *Perception, 6*, 113-119.

Kreiner, WA (2004). Size illusions as a phenomenon of limited information processing capacity. *Z. Phys. Chem.,*218, 1041-1061.

Kreiner, WA (2008). Visual illusions: subjective contours triggered by border lines below the resolution limit. *FENS Abstr., vol.4, 192.14, 2008.*

Kreiner, WA (2009). Sonne, Mond und Ursa Major – ein informationstheoretisches Modell zur Größenwahrnehmung. http://vts.uni-ulm.de/doc.asp?id=6790.

Kreiner, WA (2009). Ein mathematisches Modell zur Längenwahrnehmung – Stab mit Kugeln. http://vts.uni-ulm.de/doc.asp?id=6982.

Kreiner, WA (2011). A variant of the Baldwin illusion—Influence of orientation and gaps. *Perception, 40*, ECVP Abstract Supplement, 169.

Kreiner, WA (2012). Variants of the Baldwin illusion. http://vts.uni-ulm.de/doc.asp?id=8299.

Kreiner, WA (2012). Dependence of the Poggendorff illusion on the orientation of the stimulus. http://vts.uni-ulm.de/doc.asp?id=8292.

Kreiner, WA (2012). Ingoing versus outgoing wings. The Müller-Lyer and the mirrored triangle illusion. http://vts.uni-ulm.de/doc.asp?id=8308.

Kreiner, WA (2012). Subjective contours triggered by border lines below the resolution limit. http://vts.uni-ulm.de/doc.asp?id=8314

Li, C-Y, and Guo, K (1995). Measurement of Geometric Illuisons, illusory contours and stereo-depth at luminance and colour contrast. *Vision Res.,* 12, 1713-17

Müller-Lyer, F C (1889). Optische Urteilstäuschungen. *Archiv für Anatomie und Physiologie, Physiologische Abteilung,2,* 263-270.

Ninio, J. and O´Regan, J K (1999). Characterisation of the misalignment and misangulation components in the Poggendorff and corner-Poggendorff illusions. *Perception* 28, 949-964.

Obonai, T, & Koto-Gakko, T (1931). Experimentelle Untersuchungen über den Aufbau des Sehraumes. *Archiv für die gesamte Psychologie, 82,* 308-328.

Predebon, J (1994). The reversed Müller-Lyer illusion in conventional and in wing-amputated Müller-Lyer figures. *Psychological Research,* 56, 217-223.

Pressey, AW (1971). An extension of assimilation theory to illusions of size, area, and direction. *Perception and Psychophysics,* 9, 172-176.

Pressey, AW, Di Lollo, V, and Tait, RW (1977). Effects of gap size between shaft and fins and of angle of fins on the Müller-Lyer illusion. *Perception, 6,*435-439.

Schur, E (1925). Mondtäuschung und Sehgrößenkonstanz. *Psychologische Forschung*, 7, 44-80.

Skinner, C, and Simmons, B (1998) http://www.alma.edu/departments/psychology/SP98/BCdel/Delboeuf.html

Wallace, G.K. & Crampin, D.J. (1969). The effect of Background density on the Zöllner illusion. *Vision Res. 9*, 167-177.

Weintraub, DJ, Krantz, DH (1971). The Poggendorff illusion: Amputations, rotations, and other perturbations. *Perception and Psychophysics,* 10, 257-264.

Weintraub, DJ, Krantz, DH, and Olson, TP (1980). The Poggendorff Illusion: Consider All the Angles. *Journal of Experimental Psychology,* 6, 718-725.

Wenderoth, P, Beh, H, and White D (1978). Perceptual distortion of an oblique line in the presence of an abuttung vertical line. *Vision Research,* 18, 923-930.

Wilson, AE, Pressey, AW (1988). Contrast and assimilation in the Baldwin illusion. *Percept Mot Skills, 66*, 195-204.

Yanagisawa, N (1939). Reversed illusion on the Müller-Lyer illusion. *Japanese Journal of Psychology,*14, 321-326.

Zöllner, F (1860). Ueber eine neue Art von Pseudoskopie und ihre Beziehungen zu den von Plateau und Oppel beschrieben Bewegungsphaenomenen. *Annalen der Physik, 186*, 500-525.